AFRL-RV-PS-
TR-2011-0205
AFRL-RV-PS-
TR-2011-0205

EXPLOITING OSPaN (OPTICAL SOLAR PATROL NETWORK) DATA TO UNDERSTAND LARGE-SCALE SOLAR ERUPTIONS IMPACTING SPACE WEATHER

Edward W. Cliver

28 December 2011

Final Report

APPROVED FOR PUBLIC RELEASE; DISTRIBUTION IS UNLIMITED.

AIR FORCE RESEARCH LABORATORY
Space Vehicles Directorate
3550 Aberdeen Ave SE
AIR FORCE MATERIEL COMMAND
KIRTLAND AIR FORCE BASE, NM 87117-5776

DTIC COPY

NOTICE AND SIGNATURE PAGE

AFRL-RV-PS-TR-2011-0205 HAS BEEN REVIEWED AND IS APPROVED FOR PUBLICATION IN ACCORDANCE WITH ASSIGNED DISTRIBUTION STATEMENT.

//signed//	//signed//
Edward Cliver, RVBXS Project Manager	Joel Mozer Chief, AFRL/RVB

REPORT DOCUMENTATION PAGE

Form Approved
OMB No. 0704-0188

1. REPORT DATE *(DD-MM-YYYY)*	**2. REPORT TYPE**	**3. DATES COVERED** *(From - To)*
28-12-2011	Final Report	1 Oct 2007 – 30 Sep 2011

4. TITLE AND SUBTITLE
Exploiting OSPaN (Optical Solar Patrol Network) Data to Understand Large-Scale Solar Eruptions Impacting Space Weather

5a. CONTRACT NUMBER

5b. GRANT NUMBER

5c. PROGRAM ELEMENT NUMBER
61102F

6. AUTHOR(S)
Edward W. Cliver

5d. PROJECT NUMBER
2301

5e. TASK NUMBER

5f. WORK UNIT NUMBER
837054

7. PERFORMING ORGANIZATION NAME(S) AND ADDRESS(ES) AND ADDRESS(ES)

Air Force Research Laboratory
Space Vehicles Directorate
3550 Aberdeen Ave SE
Kirtland AFB, NM 87117-5776

8. PERFORMING ORGANIZATION REPORT NUMBER
AFRL-RV-PS-TR-2011-0205

9. SPONSORING / MONITORING AGENCY NAME(S) AND ADDRESS(ES)

10. SPONSOR/MONITOR'S ACRONYM(S)
AFRL/RVBXS

11. SPONSOR/MONITOR'S REPORT NUMBER(S)

12. DISTRIBUTION / AVAILABILITY STATEMENT

Approved for public release; distribution is unlimited. (377ABW-2011-1527 dtd 26 Oct 2011)

13. SUPPLEMENTARY NOTES

14. ABSTRACT

Observations from the prototype Optical Solar Patrol Network [OSPaN; now called ISOON (Improved Solar Optical Observing Network)] telescope at the National Solar Observatory/Sacramento Peak were analyzed to gain insight on the origin and dynamics of eruptive solar events. Solar eruptions, or coronal mass ejections (CMEs), and their associated shock waves are principal drivers of harmful space weather effects on Air Force command, control, and communications systems. Understanding how such eruptions arise and evolve is an essential step to mitigating their impacts. ISOON Hα images were compared with observations at other wavelengths for two eruptive solar events (on 11 June 2003 and 6 December 2006). These analyses provided evidence that: (1) large-scale solar waves are driven by CMEs; (2) the angular orientation of newly emerged magnetic flux on the solar surface relative to stable filaments plays a role in how rapidly the filaments are destabilized and erupt; and (3) intense decimetric radio bursts (attributed to the electron-cyclotron-maser emission mechanism) arise in low-density cavities, caused by field-aligned potential drops, in post-eruption magnetic loops on the Sun. These results demonstrate the potential of exploiting ISOON observations to increase our understanding of solar eruptions, a requirement for improved prediction and mitigation of space weather.

15. SUBJECT TERMS
Sun, Solar Flares, Coronal Mass Ejections, Solar Moreton Waves, Solar Spike Bursts; Disappearing Solar Filaments

16. SECURITY CLASSIFICATION OF:			**17. LIMITATION OF ABSTRACT**	**18. NUMBER OF PAGES**	**19a. NAME OF RESPONSIBLE PERSON**
					Edward Cliver
a. REPORT	**b. ABSTRACT**	**c. THIS PAGE**	Unlimited	24	**19b. TELEPHONE NUMBER** *(include area code)*
Unclassified	Unclassified	Unclassified			

This page is intentionally left blank.

Table of Contents

List of Figures

1. Summary

Observations from the prototype Optical Solar Patrol Network (OSPaN) telescope at the National Solar Observatory/Sacramento Peak were examined to gain insight on the origin and dynamics of eruptive solar events. [OSPaN is currently referred to as the Improved Solar Optical Observing Network (ISOON).] Solar eruptions, or coronal mass ejections (CMEs), and their associated shock waves are principal drivers of harmful space weather effects on Air Force command, control, and communications systems. Understanding how such eruptions arise and evolve is an essential step to mitigating their impacts. ISOON Hα images were compared with observations recorded at other wavelengths (e.g., radio and extreme-ultraviolet) for two eruptive solar events (on 2003 June 11 and 2006 December 6). These analyses provided evidence that: (1) large-scale solar waves are driven by CMEs; (2) the angular orientation of newly emerged flux on the solar surface relative to a stable filaments plays a role in how rapidly the filament is destabilized and erupts; and (3) intense solar decimetric radio bursts (attributed to the electron-cyclotron-maser emission mechanism) arise in low-density cavities, caused by field-aligned potential drops, in post-eruption magnetic loops on the Sun. These results indicate the potential of exploiting ISOON observations to increase our understanding of solar eruptions, a requirement for improved prediction and mitigation of space weather.

2. Introduction

Space weather is becoming increasingly important to modern society as technology advances. A recent report commissioned by the Space Studies Board of the National Research Council of the American Academy of Sciences (http://lasp.colorado.edu/education/ journalists/solar_dynamics_ws/papers/lowres%20Severe%20Space%20Weather%20 FINAL.pdf) estimated that a solar event comparable to the Carrington 1859 event (Cliver and Svalgaard, 2004; Cliver 2006) would cost the US alone on the order of $1-2 trillion due to lost economic activity. Such an event would also impact on a variety of Air Force and Department of Defense surveillance and communications systems, both ground- and space-based.

The three-year basic research effort, funded by the Air Force Office of Scientific Research (AFOSR), that is summarized in this Final Report was aimed at using OSPaN Hα data (Neidig et al., 1998) to improve our understanding of the origins of space weather, with the ultimate goal of reliable prediction and effects mitigation. OSPaN is now referred to as ISOON (Improved Optical Observing Network) and the ISOON acronym will be used in this report. The proposed work had had two principal foci: (1) understanding the origin and dynamics of eruptive solar events and; (2) investigating the nature and dynamics of large-scale solar waves. We conducted studies that led to one published paper in the refereed literature in both of these areas and published a third reviewed paper on a topic that arose somewhat serendipitously regarding an unusual type of radio burst that had a well-documented space weather effect. In the next section, we will briefly summarize and excerpt the results reported in detail in each of these papers (which are Scientific Reports 1-3 under this task).

3. Methods, Assumptions, and Procedures

3.1 On the Origin of the Solar Moreton Wave of 2006 December 6

This paper by Balsubramaniam et al. (2010) was an analysis of arguably the best-observed solar Moreton wave observed to date. The Moreton wave on 2006 December 6 (Figure 1) was associated with a large eruptive flare (3B; X6.5). The wave spanned ~270º and propagated away from solar active region (AR) 10930 with an average speed of ~850 km s^{-1}. Moreton waves, first discovered ~50 years ago (Moreton, 1960; Athay & Moreton, 1961), represent the "skirt" of a coronal shock wave as it sweeps across the chromosphere, resulting in an initial depression (red-shift of the Hα line) followed by rebound (blue-shift). Twelve minutes after the wave was first observed at 18:43 UT, the disturbance (no longer directly observable as a wave-front in Hα) disrupted the large quiescent filament in the south central portion of the solar disk.

As is the case with other large-scale waves on the Sun such as radio type II bursts and EIT waves, the origin of the Moreton waves has been controversial (Warmuth, 2007; Vršnak & Cliver, 2008) with a split among scientists between two possible sources: a flare-generated pressure pulse or a high-speed coronal mass ejection (CME). The most recent studies (e.g., Chen, 2006; Gopalswamy et al., 2008; Veronig et al., 2008; Temmer et al., 2009; Muhr et al., 2010; Veronig et al., 2010; Schrijver et al., 2011) favor the CME origin, and our analysis of the 2006 December 6 event falls in this category.

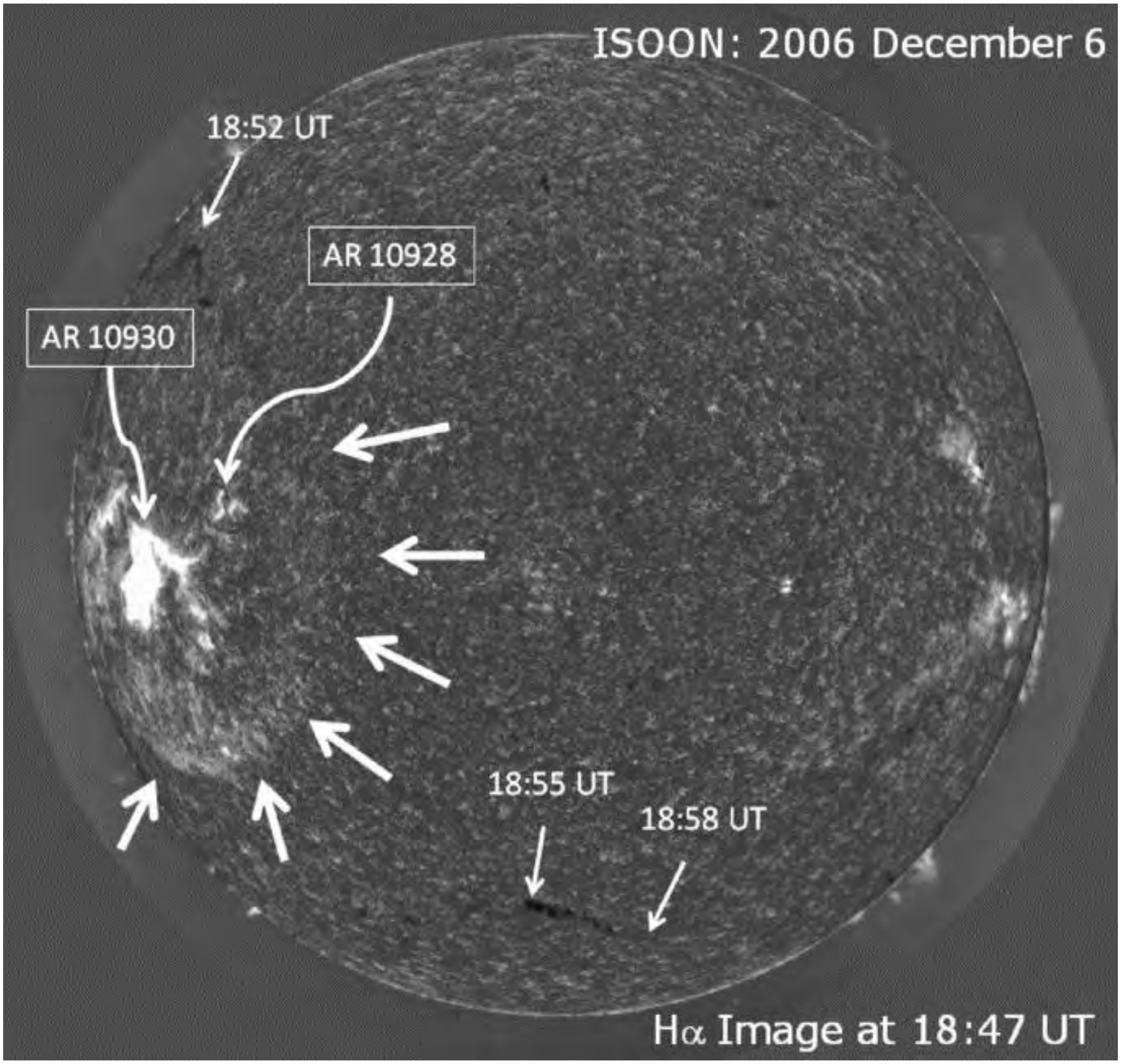

Figure 1: Overview of the Solar Eruption and Moreton Wave of 2006 December 6

In Figure 1, The Hα image was been scaled to enhance the wave. The large arrows indicate the position of the wave at 18:47 UT. The smaller arrows indicate the positions of the filaments that were disrupted by the wave at the given times as it propagated outward from AR 10930.

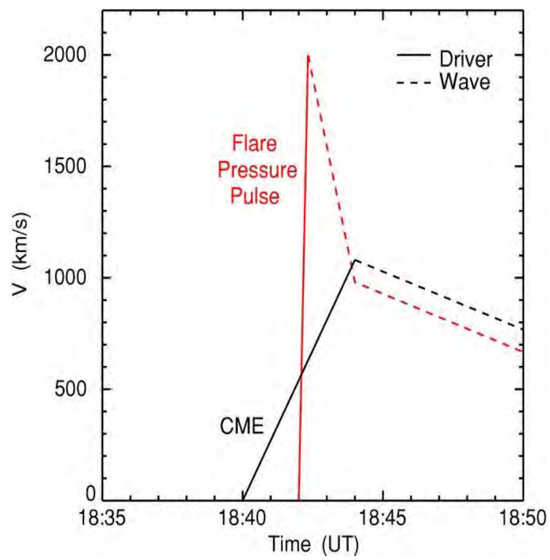

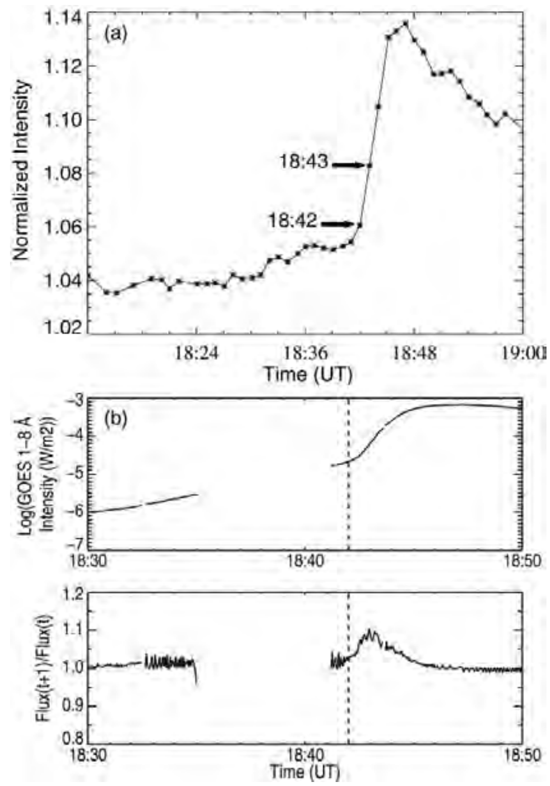

Figure 2: Time Profiles of the Modeled Lateral Velocities of the Flare Pressure Pulse and Wave (Red Solid/Dashed Line) and CME Lateral Expansion and Wave (Black Solid/ Dashed Line)

Figure 3: (Top) Normalized Hα Intensity of the 3B Flare as a Function of Time and (Bottom) GOES Intensity and Derivative

As seen at the top of Figure 3, the explosive phase was from 18:42-18:43 UT. The dashed line (center graph) represents the impulsive phase onset.

Our preference for a CME driver is based on: (a) the kinematic analysis shown in Figure 2; (b) the magnetic force profile in Figure 4; and (c) the relationship of the wave to the magnetic arcade as shown in Figure 5. The velocity profile for the pressure pulse scenario in Figure 2 is highly constrained. The onset of the flare pressure pulse is taken to be 18:42 UT based on the ISOON Hα and GOES 1-8 Å intensity curves in Figure 3. The modeled velocity profile has a rather unphysical appearance and requires extreme values of the parameters involved (pressure pulse acceleration of 100 km s^{-2} for 20 s to yield a V_O = 2000 km s^{-1}, followed by an average deceleration of -10.2 km s^{-2}) to match the observations, i.e., the wave onset time and initial distance from the radiant point and the initial measured velocity and deceleration rate. The magnetic force profile in Figure 4 was calculated from GONG magnetograph measurements at Cerro Tololo. The velocity profile for the CME scenario in Figure 2 is based on the assumption that the peak in the force (from 18:40-18:44 UT) corresponds to the cataclysmic rearrangement of magnetic field that marks the main acceleration phase of the CME. In this scenario, the velocity profile has a more natural appearance than that obtained for the flare pressure pulse driver. Figure 5 shows the relationship of the first wave contours to the magnetic arcade to the west of the main flaring region. The wave contours were obtained from the ISOON red-wing Hα observations. We argue that the eruption of this arcade of relatively weak field gave rise to the Moreton wave which appeared to form off its flanks in the south where the wave amplitude was largest.

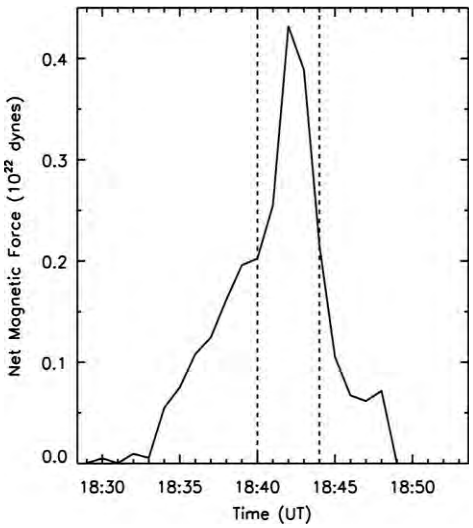

Figure 4: Time Variation of the Net Downward Lorentz Force on the Photosphere as Calculated from the Measured Longitudinal Magnetic Field Change

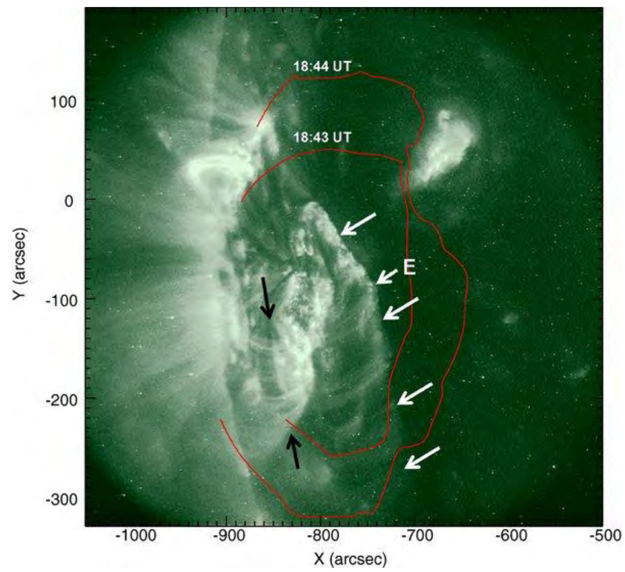

Figure 5: TRACE Image at 08:01 UT Showing the Western Arcade That We Link to the Moreton Wave (White Arrows) and the Eastern Arcade Associated with the Main Flare (Black Arrows)

In Figure 4, the vertical lines indicate the inferred time of the main acceleration phase of the CME. As seen in Figure 5, the wave contours at 18:43 and 18:44 UT (in red) conform to the boundary of the weak arcade in the south.

3.2 The Disappearing Solar Filament of 2003 June 11: A Three-body Problem

This paper by Balasubramaniam et al. (2011) examined the circumstances that led to the disruption of a large quiescent filament on 2003 June 11 (Figure 6). The disappearing solar filament (DSF) was preceded by the birth of a nearby active region (AR) 10381, first noted in Hα on June 9. The emergence of new magnetic flux in the vicinity of a filament prior to its eruption is a fairly common occurrence. What is different in this case, however, is that the filament was adjacent to an established AR (10380) and the interaction between new AR 10381 and the filament proceeded indirectly via established region 10380. Thus, we are dealing with a three-body problem. We used this unusual event to gain insight on the general question of how emerging flux disrupts solar filaments. Specifically, we asked, “What can this event tell us about how the magnetic disturbance represented by newly emerging flux ‘propagates’ to a filament? Does it take a shortest path to the chromospheric neutral line (or filament channel) or can it take a different route to the filament?”

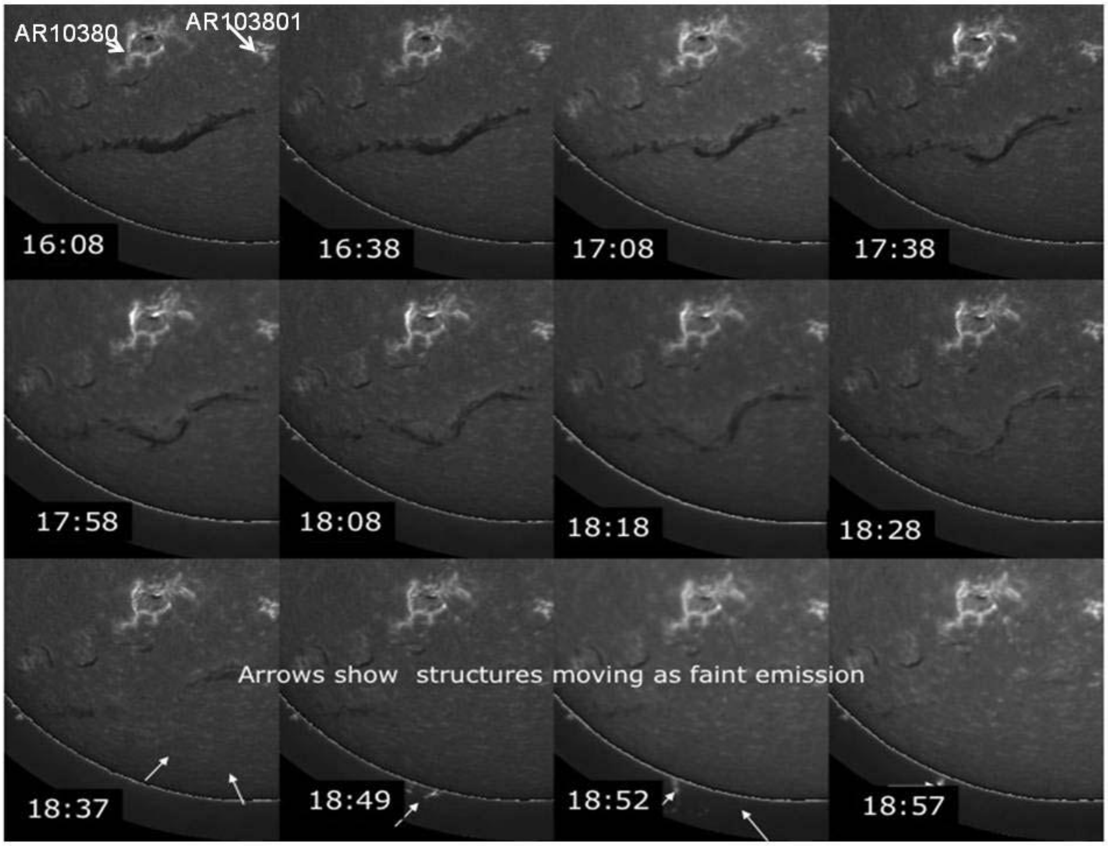

Figure 6: ISOON Telescope Images of the Disappearing Solar Filament of 2003 June 11

In Figure 6, the first frame (at 16:08 UT) shows the positions of established active region 10380 and newly formed region 10381.

As an analysis tool, we used Bruzek's empirical relationship between the distance from newly emerging flux to a filament and the time from the first observation of a new active region until filament disappearance (Figure 7). From his analysis, Bruzek (1952) obtained a typical disturbance propagation rate of 5-6 km s^{-1}. Wang & Sheeley (1999) subsequently showed that quiescent filaments were disrupted when newly emerged flux reconnected with the magnetic fields of arcades overlying the filament, thereby diverting or opening up some of the overlying field, and initiating eruption.

For the 2003 June 11 DSF, SOHO EIT images and potential field models indicate that the destabilizing disturbance from AR 10381 propagated to the filament via established region 10380. As a result of the interaction between new region 10381 and old region 10380, newly unbalanced positive polarity field in the south of 10380 reconnected with the negative polarity field on the northern flank of the filament, resulting in the divergence and removal of the overlying magnetic arcade. Figure 7 shows that if the magnetic disturbance had propagated directly from region 10381 to the filament, the data point for this event (open triangle) would have lain directly on the regression line through Bruzek's data, implying a rate of 5-6 heliographic degrees day^{-1}. Instead, the actual data point for this event (filled triangle), based on the distance from the centroid of established AR 10380 to the base of the "bulge" of the filament where the eruption originates, lies at the upper edge of the scatter, yielding a disturbance propagation rate of ~11^{o} day^{-1}. To first order, the scatter in Bruzek's plot will be affected by both the rate of new flux emergence and the strength of the "tie-down" fields over a filament. Here we suggest that the orientation of the new flux relative to the filament also plays a role. Intuitively, a broadside "attack" on the coronal fields around a filament, as was the case for the 2003 June 11 DSF (following the repositioning of the effective emerging flux as a result its interaction with the "third body"), may be more effective than an attack from one end because a larger extent of the tie-down arcade is affected. In addition, the magnetic disturbance due to newly emerging flux may not need to travel as close to the filament to destabilize it from the side, resulting in a shorter effective distance and a faster apparent propagation rate.

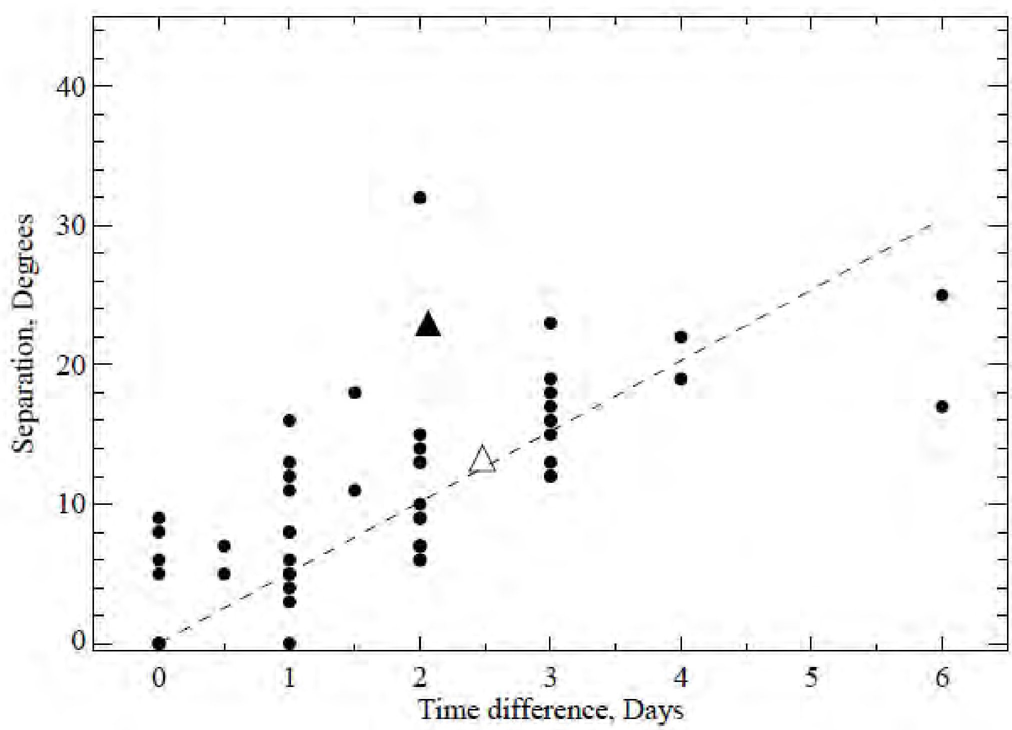

Figure 7: A Modified Version of Bruzek's (1952) Scatter Plot of the Distance Between New Active Regions and Quiescent Filaments vs. the Time Between Active Region Appearance and Filament Disappearance

In Figure 7, the filled circles represent Bruzek's data. The open triangle is based on the assumption that the magnetic disturbance propagated from region 10381 to the western tip of the filament, and the filled triangle is based on the evidence that the destabilizing disturbance propagated from 10380 (after its interaction with 10381) to the central bulge of the filament from where the eruption began. The dashed line shows a linear fit, forced to go through the origin, of Bruzek's data.

3.3 The Solar Decimetric Spike Burst of 2006 December 6: Possible Evidence for Field-aligned Potential Drops in Post-eruption Loops

In this paper by Cliver et al. (2011), we examined the origin of a large decimetric burst that caused significant signal-to-noise (S/N) degradation on Global Positioning System (GPS) receivers (Cerutti et al., 2008). The peak flux density of the L-band (1.4 GHz) burst recorded by the Owens Valley Solar Array (OVSA) in association with the 3B/X6.5 flare on 2006 December 6 (see section 2.1) was ~10^6 sfu (Gary, 2008; 1 sfu = 1 solar flux unit = 1 x 10^{-22} W m^{-2} Hz^{-1}), several times larger than the largest event previously recorded in this frequency range. The time profile of this burst is given in Figure 8, along with those of three other L-band bursts observed during solar cycle 23 that had peak intensities > 10^5 sfu.

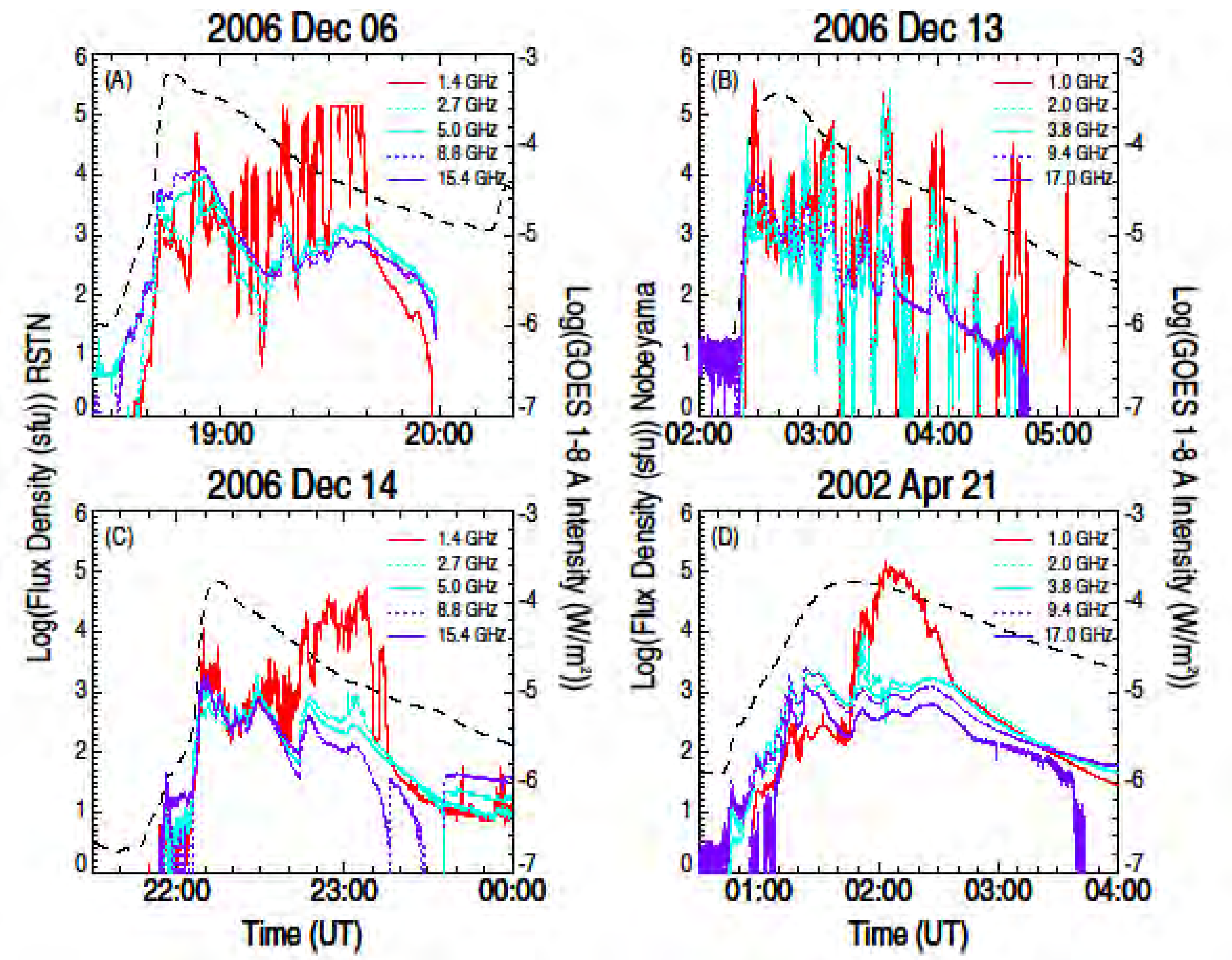

Figure 8: Great (>10^5 sfu) Decimetric Radio Bursts on (a) 2006 December 6; (b) 2006 December 13; (c) 2006 December 14; and (d) 2002 April 2

In Figure 8, the data are plotted at 1-second time resolution. For the event on December 14, OVSA recorded a burst at 1.6 GHz (not shown) with a peak intensity of ~1.5 x 10^5 sfu at 1.6 GHz.

The great decimetric burst on 2006 December 6 was also observed by the Frequency Agile Solar Radiotelescope Subsystem Testbed (FST; Liu et al. 2007) at Owens Valley. During the brightest emission in the December 6 event, the FST, which directly samples the 1.0-1.5 GHz frequency range with a Gigabit-per-second digitizer for 100 microseconds every 20 milliseconds, recorded many hundreds of intense narrowband (3-4 MHz) spike bursts per second in the GPS frequency range, with individual spikes having durations of less than 20 milliseconds (Gary 2008; Gary et al. 2011). A short sample of burst, near the time of peak intensity, is shown in Figure 9.

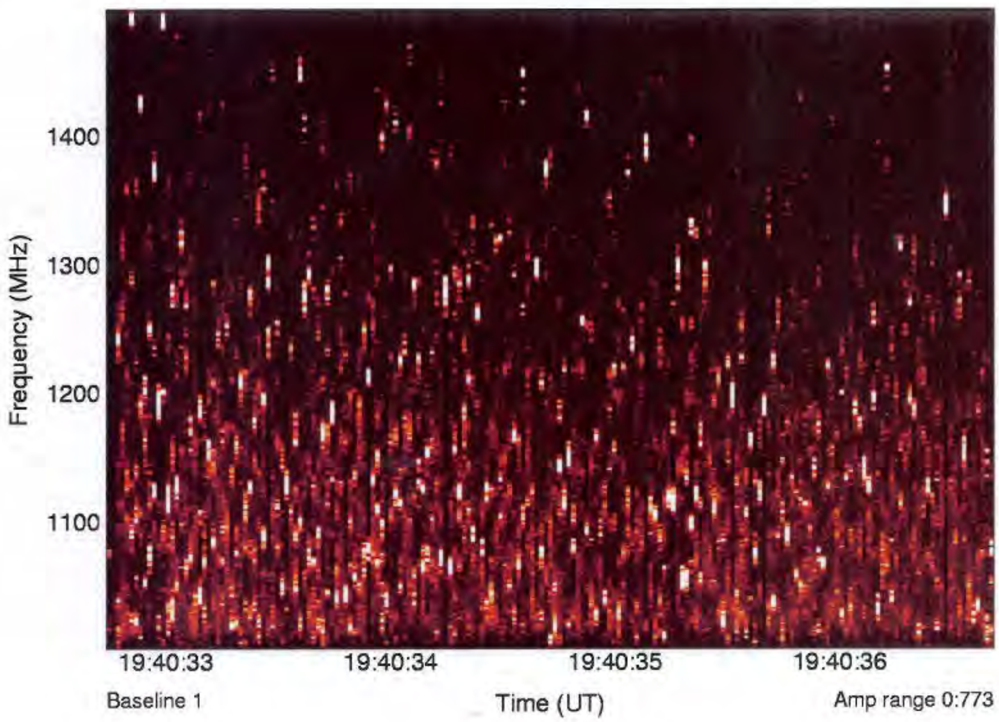

Figure 9: Detail of a FST High-Temporal- and High-Spectral-Resolution Spectrogram (for 1000-1500 MHz) for ~4 Seconds Near the End of the Most Intense Part of the Great Decimetric Burst on 2006 December 6

The extreme burst intensities in spike bursts indicate a coherent emission process, such as plasma emission (Zheleznyakov & Zaitsev 1975; Kuijpers et al. 1981) or electron cyclotron maser (ECM) emission (Wu & Lee 1979; Holman et al. 1980; Melrose & Dulk 1982). The plasma mechanism accounts for solar type III bursts while ECM emission is the favored interpretation of both Jupiter's decametric radio emission and Earth's auroral kilometric radiation (AKR) (Melrose 2009). Gary et al. (2011) interpret the spikes in the December 6 event in terms of ECM emission. Plasma emission is based on the "bump-on-tail" instability ($\partial f/\partial v_{||} > 0$) while the free energy in the ECM process is derived from positive $\partial f/\partial v_{\perp}$ (in the usual case of a loss-cone driven maser). As of yet neither the plasma nor the ECM emission mechanism has been fully successful in explaining the characteristics of solar spike bursts (e.g., Benz 1986, Messmer & Benz 2000, Battaglia & Benz 2009). The plasma hypothesis is challenged by the small bandwidths and the high brightness temperatures of decimetric spikes

(Benz 1986). The condition for ECM emission to occur (electron cyclotron frequency (f_{ce}) $\gtrsim$ plasma frequency (f_{pe}); Melrose & Dulk 1982; Benz 2004; Treumann 2006) does not apply throughout the low corona (Benz 1986, 2004), and is only likely to be satisfied either in strong-field regions just above sunspot umbrae or in low-density ducts in the low corona. The ECM emission mechanism has an additional problem at the Sun. It has long been recognized (Holman et al. 1980; Melrose & Dulk 1982) that escape of fundamental ECM emission is difficult, if not impossible, because of thermal gyro-absorption at the second harmonic in the overlying plasma. Various solutions have been proposed for this problem but none has been generally accepted. Thus both the nature of spike bursts and the escape of ECM emission at the Sun remain in question.

Surprisingly, given the intensity of the radio emission, the strongest emission in the 2006 December 6 burst and the other three events in Figure 8 favors the delayed gradual part of the event (as observed in soft X-rays), rather than the early impulsive part of the flare, generally taken to be the most energetic phase of a flare (e.g., Hudson 2011). Late phase flare phenomena such as secondary microwave peaks (Cliver, 1983) and gradual hard X-ray bursts (Cliver et al., 1986) have been attributed to particle

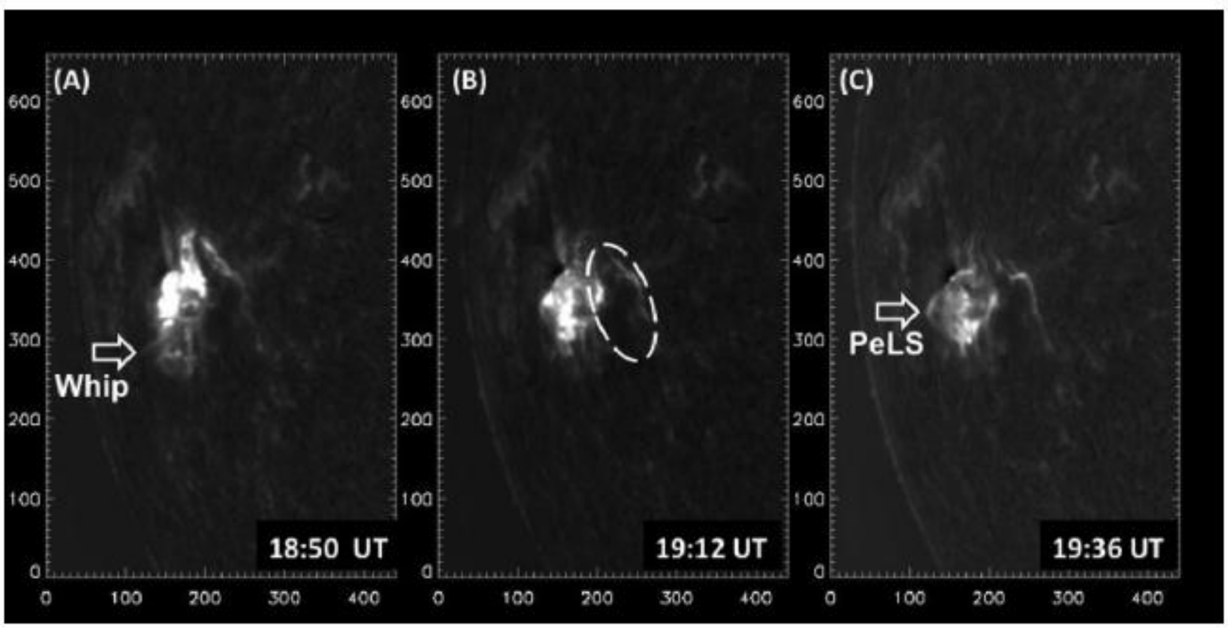

Figure 10: ISOON Hα Images at 18:50 UT (a), 19:12 UT (b), and 19:36 UT (c) of the 3B/X6 Flare on 2006 December 6

In Figure 10, the arrow in (a) points to a ray that exhibited a whip-like movement toward the south at 18:56 UT. The dashed oval in panel (b) indicates the two-ribbon flare linked to the Moreton wave analyzed by Balasubramaniam et al. (2010). The post-eruption loop system (PeLS) associated with the great decimetric burst is indicated in panel (c).

acceleration at X-type neutral points in the wake of CMEs and electron trapping on post-eruptive loop systems (PeLS). A comparison of the 1.4 GHz intensity time profile in Figure 8(a) with ISOON images in Figure 10 confirms that the peak emission comes during the time when the PeLS is most prominent.

In Cliver et al. (2011) we suggested, by analogy with AKR radio emission in Earth's magnetosphere, that the condition for ECM emission at the Sun is met for the four events in Figure 8 because of field-aligned potential drops – that give rise to density depletions – in the post-eruption loop systems observed for each of these events. Such potential drops are observed *in situ* for AKR sources in the magnetosphere. Moreover, there is a suggestion that the vertical alignment of such cavities may aid in the escape of ECM emission by ducting the radiation toward weaker magnetic field regions. A schematic depicting our view of these late intense decimetric bursts – that are linked to S/N degradation on GPS receivers – is given in Figure 11.

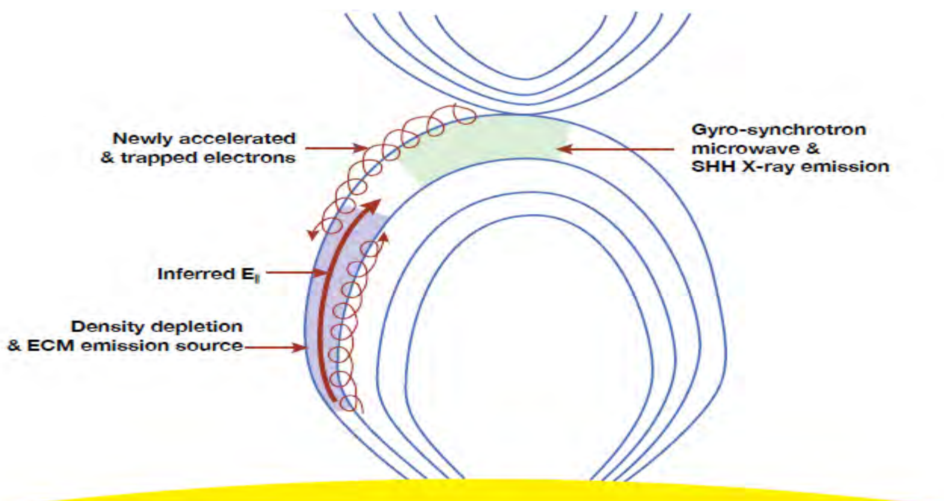

Figure 11: Schematic Showing How ECM Emission Might Arise in a Post-Eruption Loop System as a Result of Late-Phase Reconnection (Particle Acceleration) at an X-Type Neutral Point (or in a Neutral Current Sheet) and a Magnetic Field-Aligned Potential Drop (Density Depletion)

4. Results and Discussion

In this effort, we used ISOON observations, in conjunction with other space-borne and ground-based solar observations to gain insight into the eruptive solar activity that is the principal driver of severe space weather. We view the primary results of this work to be the attention that we have focused on: (1) the relationship between magnetic field changes, the impulsive phase of flares, and the main phase of CME acceleration; (2) the relative orientation of newly-emerged active regions and nearby quiescent filaments as a variable (source of scatter) in Bruzek's distance vs. time relationship connecting flux emergence with filament disappearance; and (3) a plausible scenario for ECM emission generation and escape at the Sun involving field-aligned potential drops.

While we have argued for a CME driver for the Moreton wave in the 2006 December 6 eruptive flare, the evidence is more suggestive than compelling. More definitive evidence on this point is currently being provided by the imaging assembly on board the *Solar Dynamics Observer*. In a similar vein, the suggestion that there is a connection between the rapid change of the photospheric magnetic field and the main acceleration phase of coronal mass ejections, while intriguing, will need to be substantiated using a large sample of events. The two data points for the disappearing filament on 2003 June 11 in Figure 7 suggest that the angular orientation of newly emerged flux to a stable filament should to be taken into account if one is to use the relationship in the figure to infer eruption onset. More generally, this event shows that the general magnetic environment of the filament needs to be considered. Finally, the preference for intense decimetric bursts to occur in the delayed gradual phase of flares and to (apparently) favor certain active regions opens the possibility for providing warnings for at least some GPS outages.

5. Conclusion

The Sun has been observed continuously in Hα for over 75 years. Beyond the specific results summarized and discussed in the preceding section, the work conducted under this task has demonstrated the value of the state-of-the-art ISOON patrol telescope for modern solar research, particularly when the Hα data are combined with other observations, on either side of the spectrum from the 6563 Å line. Further opportunities for exploitation of ISOON data are offered by the current fleet of space missions and the growing capabilities of ground-based radio instruments such as the pending Frequency Agile Solar Radio Telescope.

References

Athay, R. Grant, & Moreton, Gail E., "Impulsive Phenomena of the Solar Atmosphere: I, Solar Optical Events Associated with Flares Showing Explosive Phase," *Astrophysical Journal*, **133**, May 1961, pp. 935-945 (plus plates).

Balasubramaniam, K. S., Cliver, E. W., Pevtsov, A., Temmer, M., Henry, T. W., Hudson, H. S., Imada, S., Ling, A. G., Moore, R. L., Muhr, N., Neidig, D. F., Petrie, G. J. D., Veronig, A. M., Vršnak, B., & White, S. M., "On the Origin of the Solar Moreton Wave of 2006 December 6," *Astrophysical Journal*, **723**, November 2010, pp. 587-601.

Balasubramaniam, K. S., Pevtsov, A. A., Cliver, E. W., Martin, S. F., & Panasenco, A., "The Disappearing Solar Filament of 2003 June 11: A Three-body Problem," *Astrophysical Journal*, **743**, December 2011, 202 (9 pp).

Battaglia, M., & Benz, A. O., "Do Solar Decimetric Spikes Originate in Coronal X-ray Sources?," *Astronomy & Astrophysics (Letters),* **499**, June 2009, pp. L33-L36.

Benz, A. O., "Millisecond Radio Spikes," *Solar Physics*, **104**, March 1986, pp. 99-110.

Benz, A. O., "Decimeter Burst Emission and Particle Acceleration," in **Solar & Space Weather Radiophysics**, eds., D. E. Gary & C.U. Keller, Kluwer Academic Publishers, Dordrecht, 2004, pp. 203-221.

Bruzek, A., "Über die Ursache der "Plötzlichen" Filamentauflösungen," 1952, *Zeitschrift für Astrophysik,* **31**, 1952, pp. 99-110.

Cerutti, Alessandro P., Kinter, Paul M., Jr., Gary, Dale E., Mannucci, Anthony J., Meyer, Robert F., Doherty, Patricia, & Coster, Anthea J., "Effect of Intense December 2006 Solar Radio Bursts on GPS Receivers," *Space Weather*, **6**, October 2008, S10D07 (10 pp).

Chen, P. F., "The Relation Between EIT Waves and Solar Flares," *Astrophysical Journal (Letters)*, **641**, April 2006, pp. L153-L156.

Cliver, E. W., "Secondary Peaks in Solar Microwave Outbursts," *Solar Physics*, **84**, April 1983, pp. 347-359.

Cliver, E. W., Dennis, B. R., Kiplinger, A. L., Kane, S. R., Neidig, D. F., Sheeley, N. R., Jr., & Koomen, M. J., "Solar Gradual Hard X-ray Bursts and Associated Phenomena," *Astrophysical Journal,* **305**, June 1986, pp. 920-935.

Cliver, E. W., & Svalgaard, L., "The 1859 Solar-terrestrial Disturbance and the Current Limits of Extreme Space Weather Activity," *Solar Physics*, **224**, October 2004, pp. 407-422.

Cliver, E.W., “The 1859 Space Weather Event: Then and Now,” *Advances in Space Research*, **38**, 2006, pp. 119-129.

Cliver, E. W., White, S. M., & Balasubramaniam, K. S., “The Solar Decimetric Spike Burst of 2006 December 6: Possible Evidence for Field-aligned Potential Drops in Post-eruption Loops,” *Astrophysical Journal*, **740**, December 2011, 145 (8 pp).

Gary, D. E., “Cause and Extent of the Extreme Radio Flux Density Reached by the Solar Flare of 2006 December 06,” in **Ionospheric Effects Symposium (Proceedings)**, ed., J.M. Goodman, Sheridan Books, Hunt Valley, MD, 2008, pp. 18-25.

Gary, D. E., et al., “FST Observations of the Great Solar Radio Burst of 2006 December 6,” 2011 (in preparation).

Gopalswamy, N., Akiyama, S., & Yashiro, S., “Major Solar Flares Without Coronal Mass Ejections,” in **Universal Heliophysical Processes (**Proceedings of IAU Symposium 257), eds., Natchimuthukonar Gopalswamy & David F. Webb, Cambridge University Press, Cambridge, 2009, pp. 283-286.

Holman, G. D., Eichler, D., & Kundu, M. R., “An Interpretation of Solar Flare Microwave Spikes as Gyrosynchrotron Masering,“ in **Radio Physics of the Sun** (in Proceedings of IAU Symposium 86), eds., M. R. Kundu & T. E. Gergely, D. Reidel Publishing Company, Dordrecht, 1980, pp. 457-459.

Hudson, Hugh S. “Global Properties of Solar Flares,” *Space Science Reviews*, **158**, January 2011, pp. 5-41.

Kuijpers, J., van der Post, P., & Slottje, C., “Runaway Acceleration in a Radio Flare,” *Astronomy & Astrophysics*, **103**, November 1981, pp. 331-338.

Liu, Zhiwei, Gary, Dale E., Nita, Gelu M., White, Stephen M., & Hurford, Gordon J., “A Subsystem Test Bed for the Frequency-Agile Solar Radiotelescope,” *Publications of the Astronomical Society of the Pacific*, **119**, March 2007, pp. 303-317.

Melrose, D. B., “Coherent Emission,” in **Universal Heliophysical Processes** (Proceedings of IAU Symposium 257), eds., Natchimuthukonar Gopalswamy & David F. Webb, Cambridge University Press, Cambridge, 2009, pp. 305-315.

Melrose, D. B., & Dulk, George A., “Electron-cyclotron Masers as the Source of Certain Solar and Stellar Radio Bursts,” *Astrophysical Journal*, **259**, August 1982, pp. 844-858.

Messmer, Peter, & Benz, Arnold O., “The Minimum Bandwidth of Narrow Band Spikes in Solar Flare Decimetric Radio Waves,” *Astronomy & Astrophysics*, **354**, February 2000, pp. 287-295.

Moreton, G. E., “Hα Observations of Flare-initiated Disturbances with Velocities ~1000 km/s,” *Astronomical Journal*, **65**, 1960, pp. 494-495.

Muhr, N., Vršnak, B., Temmer, M., Veronig, A. M., & Magdalenić, J., “Analysis of a Global Moreton Wave Observed on 2003 October 28,” *Astrophysical Journal*, **708**, January 2010, pp. 1639-1649.

Neidig, D., Wiborg, P., Confer, M., Haas, B., Dunn, R., Balasubramaniam, K.S., Gullixson, C., Craig, D., Kaufman, M., Hull, W., McGraw, R., Henry, T., Rentschler, R., Keller, C., Jones, H., Coulter, R., Gregory, S., Schimming, R., & Smaga, B., “The USAF Improved Solar Observing Optical Network (ISOON) and its Impact on Solar Synoptic Data Bases,” in **Synoptic Solar Physics** (Proceedings of ASP Conference 140), eds., K. S. Balasubramaniam, J. Harvey, & D. Rabin, Astronomical Society of the Pacific, San Francisco, 1998, pp. 519-528.

Schrijver, Carolus J., Aulanier, Guillaume, Title, Alan M., Pariat, Etienne, & Delannée, Cecile, “The 2011 February 15 X2 Flare, Ribbons, Coronal Front, and Mass Ejection: Interpreting the Three-dimensional Views from the *Solar Dynamics Observatory* and *STEREO* Guided by Magnetohydrodynamic Flux-rope Modeling,” *Astrophysical Journal*, **738**, September 2011, 167 (23 pp).

Temmer, M., Veronig, A.M., Vršnak, B., Rybák, J., Gömöry, P., Stoiser, S., & Marićić, D., “Acceleration in Fast Halo CMEs and Synchronized Flare HXR Bursts,” *Astrophysical Journal (Letters)*, **673**, January 2008, pp. L95-L98

Treumann, Rudolf A., “The Electron-cyclotron Maser for Astrophysical Application,” *Astronomy & Astrophysics Review,* **13**, August 2006, pp. 229-315.

Veronig, Astrid M., Temmer, Manuela, & Vršnak, Bojan, “High-cadence Observations of a Global Coronal Wave by *STEREO* EUVI,” *Astrophysical Journal (Letters)*, **681**, pp. L113-L116.

Veronig, A. M., Muhr, N., Kienreich, I. W., Temmer, M., & Vršnak, B., “First Observations of a Dome-shaped Large-scale Coronal Extreme-ultraviolet Wave,” *Astrophysical Journal (Letters),* **716**, June 2010, pp. L57-L62.

Vršnak, Bojan, & Cliver, Edward W. 2008, “Origin of Coronal Shock Waves (Invited Review),” *Solar Physics*, **253**, December 2008, pp. 215-235.

Wang, Y. M., & Sheeley, N. R., Jr., Filament Eruptions Near Emerging Bipoles,” *Astrophysical Journal*, **510**, January 1999, pp. L157-L160.

Warmuth, Alexander, “Large-scale Waves and Shocks in the Solar Corona,” in **The High Energy Solar Corona: Waves, Eruptions, Particles** (Lecture Notes in Physics 725), eds., Karl-Ludwig Klein & Alexander L. MacKinnon, Springer-Verlag, Berlin, 2007, pp. 107, pp. 107-138.

Wu, C. S., & Lee, L. C., “A Theory of the Terrestrial Kilometric Radiation,” *Astrophysical Journal*, **230**, June 1979, pp. 621-626.

Zheleznyakov, V. V., & Zaitsev, V. V., “Some Features of Solar Spike Burst Generation,” *Astronomy & Astrophysics,* **39**, February 1975, pp. 107-111.

DISTRIBUTION LIST

DTIC/OCP 8725 John J. Kingman Rd, Suite 0944 Ft Belvoir, VA 22060-6218	1 cy
AFRL/RVIL Kirtland AFB, NM 87117-5776	2 cys
Official Record Copy AFRL/RVBXS/Edward Cliver	1 cy

This page intentionally left blank.